Copy
RM L53C17

NACA

RESEARCH MEMORANDUM

LARGE-SCALE FLIGHT MEASUREMENTS OF ZERO-LIFT DRAG AND

LOW-LIFT LONGITUDINAL CHARACTERISTICS OF A

DIAMOND-WING—BODY COMBINATION AT MACH

NUMBERS FROM 0.725 TO 1.54

By Harvey A. Wallskog and John D. Morrow

Langley Aeronautical Laboratory
Langley Field, Va.

NATIONAL ADVISORY COMMITTEE
FOR AERONAUTICS

WASHINGTON
April 20, 1953

319,98/13

NATIONAL ADVISORY COMMITTEE FOR AERONAUTICS

RESEARCH MEMORANDUM

LARGE-SCALE FLIGHT MEASUREMENTS OF ZERO-LIFT DRAG AND

LOW-LIFT LONGITUDINAL CHARACTERISTICS OF A

DIAMOND-WING—BODY COMBINATION AT MACH

NUMBERS FROM 0.725 TO 1.54

By Harvey A. Wallskog and John D. Morrow

SUMMARY

A large-scale diamond-wing—body configuration has been flown by the Langley Pilotless Aircraft Research Division at Mach numbers from 0.725 to 1.54 and Reynolds numbers, based on the wing mean aerodynamic chord, up to 35×10^6. The diamond-plan-form wing had an NACA 65A003 airfoil section, a total aspect ratio of 2.31, and 0° sweep of the mid-chord. Coefficients of total drag, base drag, model fore drag, and wing-plus-interference drag at zero lift were obtained for the Mach number range indicated, along with lift coefficients, aerodynamic-center locations, damping factors, and lift-drag ratios for two transonic Mach numbers at low-lift conditions. Drag-coefficient values of a 3-percent-thick 60° delta-wing configuration are shown for comparison.

Both total and wing-plus-interference drag coefficients for the diamond-wing model were slightly lower than for the delta-wing model at high subsonic and transonic speeds. Wing-plus-interference drag coefficients of the diamond wing were approximately 50 percent greater than those of the delta wing for Mach numbers over 1.3. Total configuration drag coefficients of the diamond-wing model, however, were only about 17 percent greater than those for the delta wing at Mach numbers above 1.3.

INTRODUCTION

The Langley Pilotless Aircraft Research Division is conducting a research program to determine the zero-lift drag of large-scale rocket-propelled wing-body configurations. This program is directed toward the design of aircraft configurations suitable for efficient flight at

transonic and supersonic speeds. A summary of the results obtained thus far in this program is given in reference 1 which presents the data obtained from 10 wing-body configurations in which the main variables were wing plan form and airfoil section.

As a continuation of this program another plan form has been investigated. As illustrated in reference 1, a thin 60° delta wing possesses an advantage of low zero-lift drag. But this delta wing, and other thin swept wings, has the disadvantage of being subject to undesirable aeroelastic effects. It seemed desirable, therefore, to obtain large-scale drag data for a wing which would have reasonably low drag and yet be free of large aeroelastic effects. The wing tested had the same wing aspect ratio, taper ratio, airfoil section, and ratio of body frontal area to wing area as a previously reported 60° delta-wing configuration but with 0° sweep of the 50-percent-chord line. This gave, essentially, an unswept wing of zero taper ratio with an inherently higher lift-curve slope than the delta wing.

This paper, then, reports the results of a free-flight test of a configuration having a diamond-plan-form wing of aspect ratio 2.31 with 0° sweep of the midchord, and an NACA 65A003 airfoil section mounted on a parabolic body having a fineness ratio of 10.

This free-flight test provided continuous measurement of longitudinal and normal accelerations, angles of attack, and base pressures by means of telemetry. From these data the variations of total drag and base pressure coefficients with Mach number were obtained. By using two small rockets in the body nose, the model was twice caused to oscillate freely in pitch during its deceleration from supersonic speeds. Telemetered values of time histories of normal acceleration and angle of attack provided lift-curve slope, static stability, and damping derivatives. The drag of the diamond-wing configuration of this investigation is compared with that of a 60° delta-wing model (model 3 of ref. 1).

The Reynolds numbers of the present test, based on wing mean aerodynamic chord, varied from 11.5×10^6 to 35×10^6. The Mach number range was from 0.725 to 1.54.

SYMBOLS

C_D drag coefficient at zero lift, Drag/qS_w

C_{p_b} body base pressure coefficient, $\dfrac{p_b - p_0}{q}$

p_b	body base pressure, lb/sq ft
p_0	atmospheric pressure, lb/sq ft
q	dynamic pressure, $\frac{1}{2}\rho V^2$, lb/sq ft
M	Mach number
R	Reynolds number
ρ	air density, slugs/cu ft
V	model airspeed, ft/sec
Λ	wing sweepback angle, $0°$ at midchord, $40° 54'$ at leading edge
A	wing aspect ratio (2.31), b^2/S_w
b	wing span, 5.64 ft
c	wing local chord, ft
$\bar{c}$	mean aerodynamic chord, 3.42 ft
c_r	wing root chord, 5.13 ft
c_t	wing tip chord, 0 ft
X	axial distance along body from nose, ft
l	total body length, ft
S_w	wing-plan-form area obtained by extending the leading and trailing edges of the wing to the center line of the body, 15.13 sq ft
S_f	body frontal area, 0.922 sq ft
a	cross-sectional area of the configuration at any longitudinal station, sq ft
C_L	lift coefficient, Lift/qS_w
C_m	pitching-moment coefficient, $\text{Moment}/qS_w\bar{c}$
$\left(C_{m_q} + C_{m_{\dot{\alpha}}}\right)$	rotational damping-moment coefficient (stable when negative), radians

α angle of attack, deg

θ angle of pitch, radians

Subscripts:

$$\dot{\alpha} = \frac{d\alpha}{dt} \frac{\bar{c}}{2V} 57.3$$

$$q = \frac{d\theta}{dt} \frac{\bar{c}}{2V}$$

The symbols α, q, and $\dot{\alpha}$ used as subscripts indicate the derivative of the quantity with respect to the subscript.

MODEL AND TESTS

Figure 1 gives the general arrangement and geometry of the present configuration. The diamond-plan-form wing had an aspect ratio of 2.31 and an NACA 65A003 airfoil section, as did a previously reported 60° delta wing (model 3 of ref. 1), and had 0° sweep of the midchord. The wing was so located on the body that the quarter-chord point of the mean aerodynamic chord fell at the 60-percent-body station. The parabolic body had its profile defined by two parabolic arcs each having its vertex at the maximum diameter which was at the 40-percent-body station. A table of fuselage coordinates may be found in reference 1. The model was stabilized by thin tail fins, four on the model without wings and two on the model with wings.

The model was constructed primarily of wood and reinforced with metal. A 6-inch ABL Deacon rocket motor furnished a total impulse of 19,000 pound-seconds which propelled the model to supersonic speeds. Two small rockets were located in the nose of the body and arranged so that their discharge, during free flight, caused the model to pitch. These "pulse rockets" had a very short burning time and served only as an initial disturbance; the model thereafter described a free oscillation. Each of the pulse rockets had a total impulse of approximately 20 pound-seconds. The model was launched, as shown in figure 2, at an elevation angle of approximately 65° and the data were measured during the coasting period of flight.

The test model had a 4-channel telemeter contained within the body which measured longitudinal acceleration, normal acceleration, base pressure, and angle of attack. Ground instrumentation was also used to

record the model flight and consisted of a CW Doppler velocimeter radar
for measuring model speed, an NACA modified SCR 584 radar tracking unit
for measuring trajectory, and radiosonde units for measuring air pres-
sure and temperature from which speed of sound, density, viscosity, and
altitude were obtained. The CW Doppler radar unit provides measurements
of model speed relative to the ground. In order to obtain the velocity
of the model relative to the air, it is necessary to know the wind speed
and direction at altitude. Wind velocities for each model have been
estimated by the Meteorology Section of the Langley Flight Research
Division by using winds-aloft data obtained at nearby weather stations.
By means of these wind data, the measured model ground speeds were then
adjusted to airspeeds. For determining drag coefficients, decelerations
were obtained from two independent sources: (a) telemetry of longitudinal
acceleration and (b) differentiation of the velocity-time curve (obtained
from the CW Doppler velocimeter). When abrupt changes occurred in the
variation of drag with Mach number, the data obtained from the telemeter,
which is more sensitive to such abrupt changes than the velocimeter
recording system, were used to guide the faired curves. Base pressure
coefficients were determined from the radiosonde survey of air pressure
and telemetered values of pressure at the base periphery.

The probable errors in the data presented due to inaccuracies in
the instruments and in the reduction of instrument recorded data and to
the errors in obtaining winds-aloft data are believed to be less than
±0.010 in Mach number and ±0.0007 in drag coefficient.

The Reynolds number based on the mean aerodynamic chord of the wing
is shown as a function of Mach number in figure 3.

RESULTS AND DISCUSSION

Zero-Lift Drag

In figure 4 are presented basic data as coefficients of total and
base drag, and base pressure against Mach number. The base-pressure-
coefficient curve in figure 4(b) is a true reproduction of the actual
data; however, it is believed that these abrupt changes are the result
of rocket-motor afterburning. These changes in base pressure coefficient,
when converted to base drag coefficient, amounted to less than the
probable error in total drag coefficient; therefore, both total drag and
base drag are presented as faired curves. The base drag of the diamond-
wing—body configuration was only 6 percent of the total drag at super-
sonic speeds.

A comparison of the present test results with those of a previously
reported 3-percent-thick 60° delta-wing model (model 3 of ref. 1) is

shown in figure 5. The diamond-wing configuration (fig. 5(a)) had
slightly lower drag than the delta-wing configuration up to a Mach
number of 1.02. Above a Mach number of 1.3, the diamond-wing configura-
tion had approximately 17 percent more drag than the delta-wing config-
uration. The drag rise of the diamond-wing configuration occurred at
a slightly higher Mach number than that of the delta-wing configuration.

In figure 5(b) a comparison of wing-plus-interference drag coeffi-
cient for the delta and diamond wings is shown. The diamond wing had
lower wing-plus-interference drag coefficients up to a Mach number of 1.02.
Above a Mach number of 1.3 the diamond wing had about 50 percent more
wing-plus-interference drag than the delta wing. The shape of the curve
for the diamond wing is typical of that for round-nose unswept wings which
generally show an approximately constant drag-coefficient variation with
Mach number for supersonic speeds.

The diamond-plan-form wing may be considered as being derived from
the delta wing by shearing the airfoil sections parallel to the fuselage
center line forward until the 50-percent-chord line has $0°$ sweep. Since
both wings have the same airfoil section, a spanwise line of a given
percentage chord will define the same streamwise surface slope for both
wings. The important consideration in comparing wing drag coefficients
is the fact that the lines of appreciable slope contributing to the drag
all have moderate sweep for the diamond wing, whereas part of the delta
wing has very little sweep (that is, the trailing-edge part). The higher
transonic drag of the delta wing is believed to be the result of low
trailing-edge sweep; whereas, the drag of the diamond wing is lower
because both the leading and trailing edges have moderate sweep. At
supersonic speeds the leading-edge portion of the wings appears to be
the predominant factor for drag. The delta wing, with its greater leading-
edge sweep, therefore has lower supersonic drag.

As shown in reference 2 the zero-lift drag rise of wing-body com-
binations at transonic speeds is related to the longitudinal distribution
of cross-sectional area. Illustrated in figure 6 are the distributions
of area for the diamond- and delta-wing configurations of this report
which, for purposes of comparison, are considered to represent equivalent
bodies of revolution. Although it would be rather difficult to predict
the total drag of each configuration, it may be possible to note the
probable sources of the drag differences by a comparison of the area dis-
tributions. The earlier drag rise of the delta-wing—body model is proba-
bly related to the higher rate of decrease of cross-sectional area of
the afterbody for the delta model as compared with that for the diamond
in the region behind $0.75 \frac{X}{l}$. As shown in reference 3, more convergent
afterbodies will have an earlier drag rise and a decreasing drag with
increasing supersonic Mach number. The higher supersonic drag of the

diamond-wing model may be, in part, the result of slightly larger maximum frontal area, greater forebody slope in the region of $0.55 \frac{X}{l}$, and, perhaps, because the afterbody drag of the diamond remains more nearly constant with increasing Mach number.

Low-Lift Longitudinal Characteristics

The static stability and damping of the model was determined by the free-oscillation method of analysis of reference 4. Illustrated in figure 7 is a portion of the time history of the data obtained from the present model in free flight showing the motions due to a pulse-rocket disturbance. Values of lift coefficient plotted against angle of attack, at two transonic Mach numbers, are presented in figure 8. The variation of C_L with α was linear for the range of these tests. The lift-curve slope was 0.070 at $M = 1.13$ and 0.067 at $M = 1.01$.

A summary of the longitudinal characteristics of the diamond-wing model obtained in this investigation is presented in table I. The static stability was determined from the measured periods of oscillation. The aerodynamic-center location moved forward from 33.1 percent of the mean aerodynamic chord at a Mach number of 1.13 to 27.0 percent of the mean aerodynamic chord at a Mach number of 1.01. The damping factor $C_{m_q} + C_{m_{\dot\alpha}}$, as obtained from the time to damp to one-half amplitude, showed a very small unstable damping-moment coefficient at $M = 1.13$.

Maximum lift-drag ratios and the lift coefficients at which they occur are also listed in table I for the diamond-wing configuration. The maximum lift-drag ratio for the delta-wing—body combination was estimated from unpublished data at a Mach number of 1.13 and was found to be about 10 percent lower than that for the diamond-wing model. These estimates for the delta-wing configuration show $(L/D)_{max} = 6.7$ and C_L for $(L/D)_{max} = 0.24$ at $M = 1.13$, while the corresponding estimates for the diamond-wing configuration were 7.35 and 0.275, respectively.

CONCLUSIONS

A diamond-plan-form wing having an aspect ratio of 2.31 and an NACA 65A003 section was tested in free flight at Mach numbers from 0.725 to 1.54 and Reynolds numbers up to 35×10^6. The results of this flight test indicate the following conclusions:

1. The variation of wing-plus-interference drag coefficient with Mach number for the diamond-wing configuration was similar to that for round-nose unswept wings which usually show a nearly constant drag coefficient at supersonic speeds.

2. The diamond-wing configuration had slightly lower total drag coefficients up to $M = 1.02$ than a similar delta-wing configuration but the supersonic drag coefficient was about 17 percent greater. The wing-plus-interference drag coefficients of the diamond wing were lower than those of the delta wing at Mach numbers up to 1.02. Above a Mach number of 1.3, however, the diamond wing had about 50 percent more drag.

3. At Mach numbers 1.13 and 1.01 the slopes of the lift curves were 0.070 and 0.067 per degree, respectively, the aerodynamic-center locations were 33.1 and 27.0 percent of the mean aerodynamic chord, respectively, and the maximum lift-drag ratios were estimated to be 7.35 and 7.60, respectively.

Langley Aeronautical Laboratory,
    National Advisory Committee for Aeronautics,
        Langley Field, Va.

REFERENCES

1. Morrow, John D., and Nelson, Robert L.: Large-Scale Flight Measurements of Zero-Lift Drag of 10 Wing-Body Configurations at Mach Numbers From 0.8 to 1.6. NACA RM L52D18a, 1953.

2. Whitcomb, Richard T.: A Study of the Zero-Lift Drag-Rise Characteristics of Wing-Body Combinations Near the Speed of Sound. NACA RM L52H08, 1952.

3. Hart, Roger G., and Katz, Ellis R.: Flight Investigations at High-Subsonic, Transonic, and Supersonic Speeds To Determine Zero-Lift Drag of Fin-Stabilized Bodies of Revolution Having Fineness Ratios of 12.5, 8.91, and 6.04 and Varying Positions of Maximum Diameter. NACA RM L9I30, 1949.

4. Gillis, Clarence L., Peck, Robert F., and Vitale, A. James: Preliminary Results From a Free-Flight Investigation at Transonic and Supersonic Speeds of the Longitudinal Stability and Control Characteristics of an Airplane Configuration With a Thin Straight Wing of Aspect Ratio 3. NACA RM L9K25a, 1950.
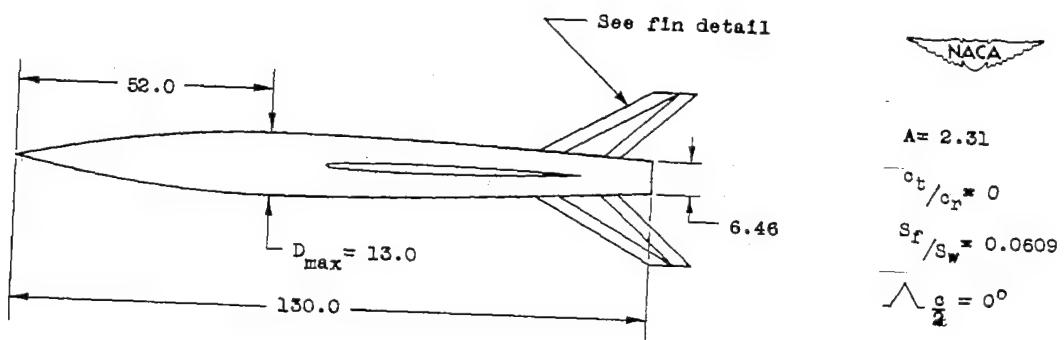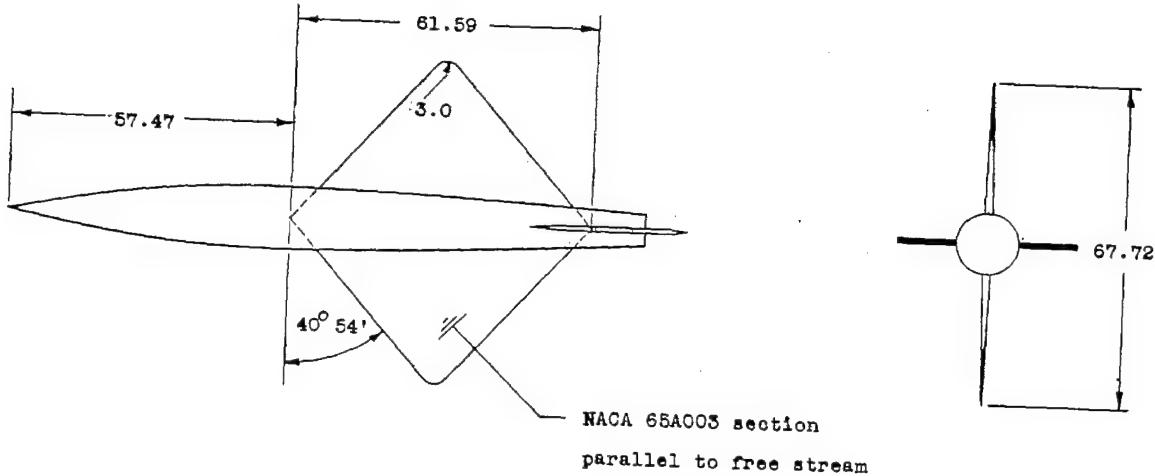
TABLE I

AERODYNAMIC CHARACTERISTICS

Aerodynamic parameter	First pulse	Second pulse
Mach number	1.13	1.01
Period, sec	0.15	0.19
C_{L_α}, per degree	0.070	0.067
Time to damp to 1/2 amplitude, sec	0.155	0.21
C_{m_α} about center of gravity, per degree	-0.0276	-0.0223
$C_{m_q} + C_{m_{\dot\alpha}}$, per radian	0.112	-0.756
Aerodynamic center, percent $\bar{c}$	33.1	27.0
$(L/D)_{max}$ (estimated)	7.35	7.60
C_L for $(L/D)_{max}$ (estimated)	0.275	0.250

61.59

57.47

3.0

40° 54'

NACA 65A003 section
parallel to free stream

67.72

See fin detail

NACA

52.0

A = 2.31

$c_t/c_r = 0$

$s_f/s_w = 0.0609$

$\bigwedge \frac{c}{2} = 0°$

$D_{max} = 13.0$

6.46

130.0
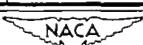
(a) Wing and body details.

Figure 1.- Geometric arrangement of the test model. All dimensions are
in inches.
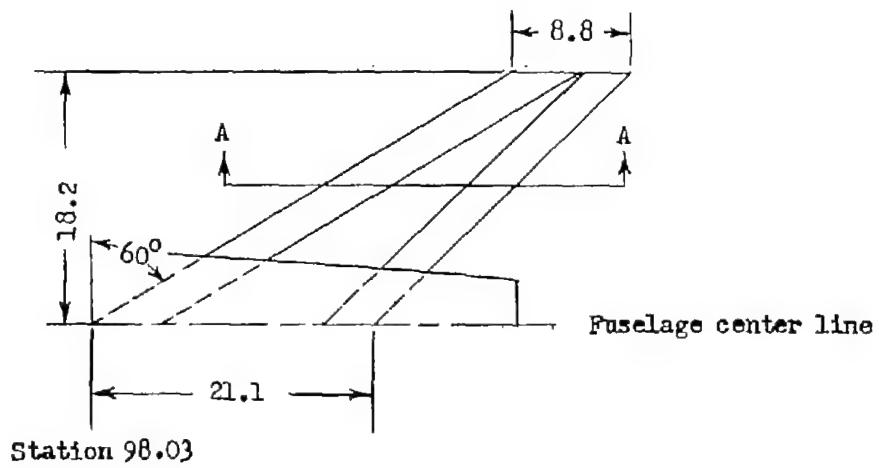
(b) Stabilizing fin details.
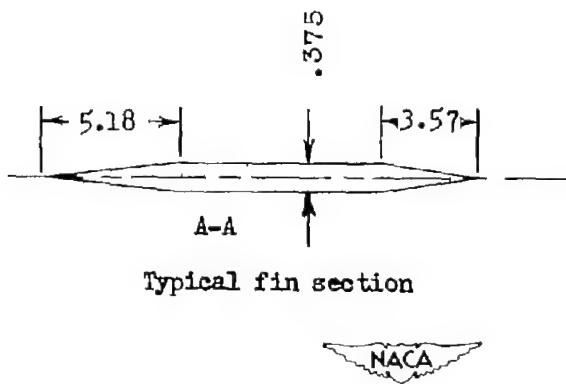
Figure 1.- Concluded.
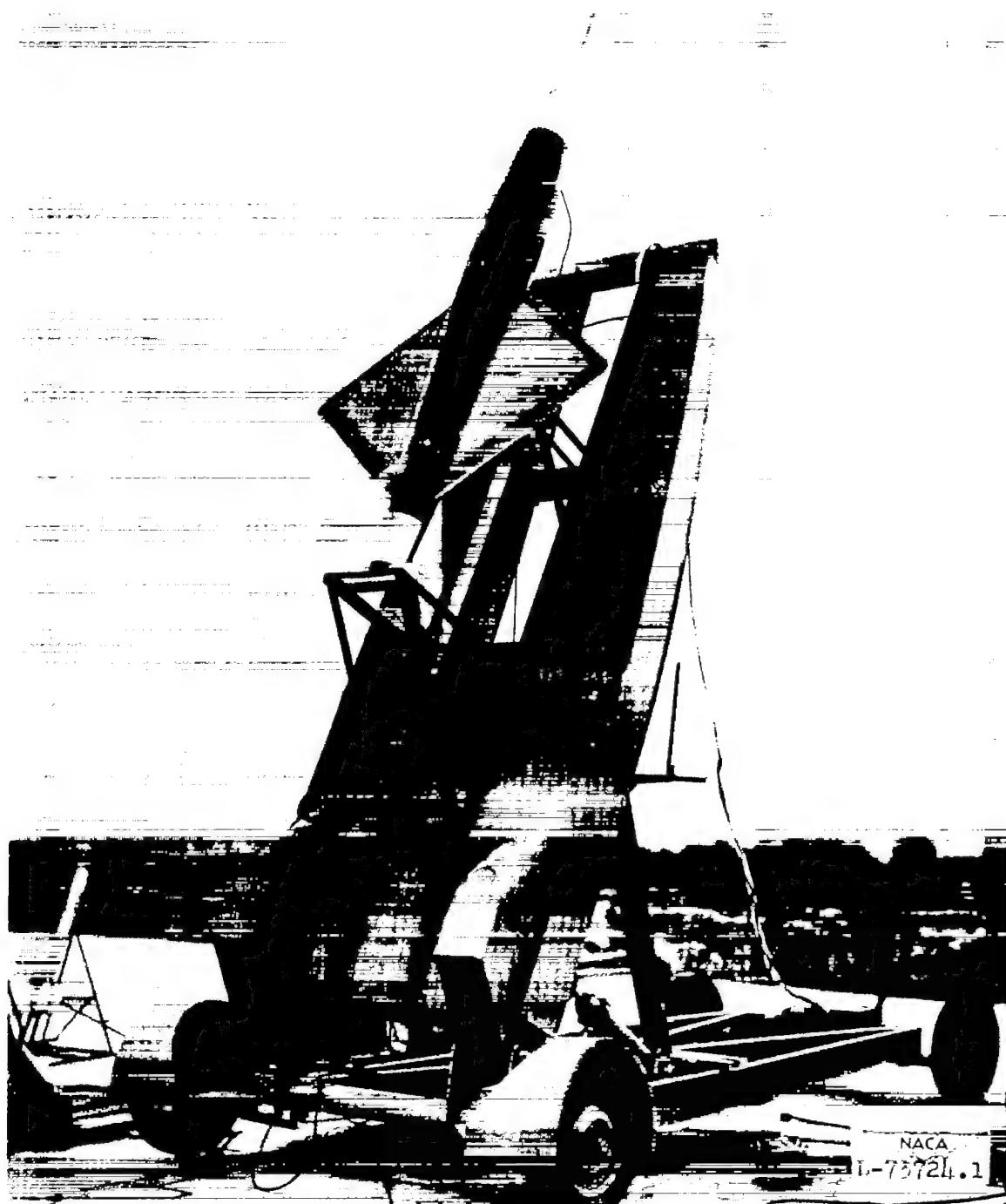
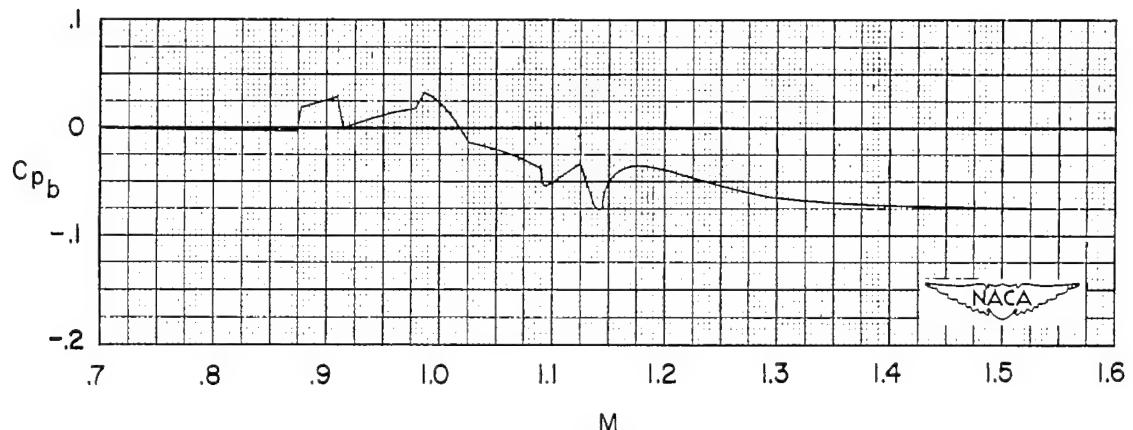Figure 2.- General view of the model on the launching stand.
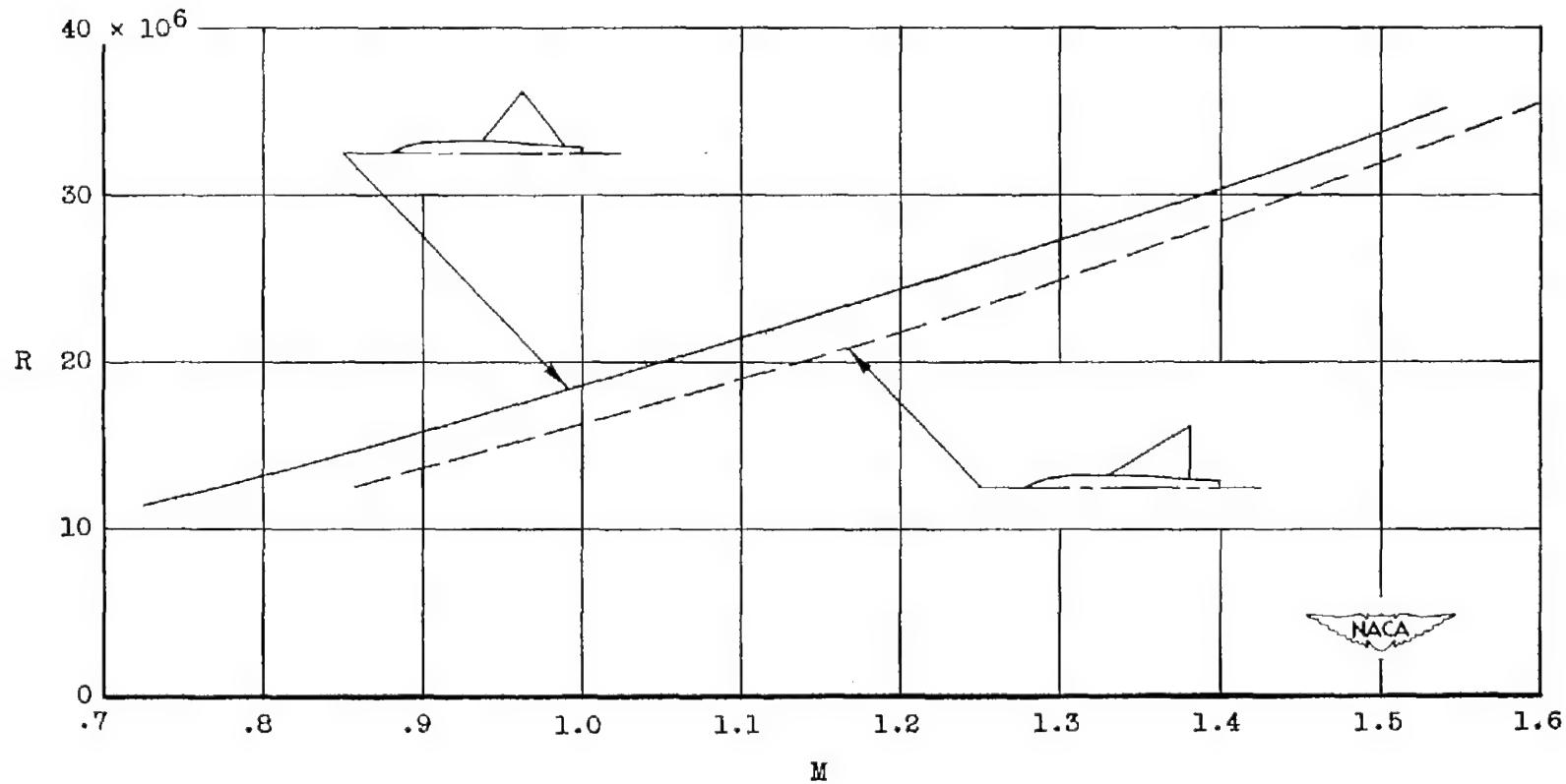
Figure 3.- Variation of Reynolds number (based on a wing mean aerodynamic chord of 3.42 feet) with Mach number for the models presented in this report.
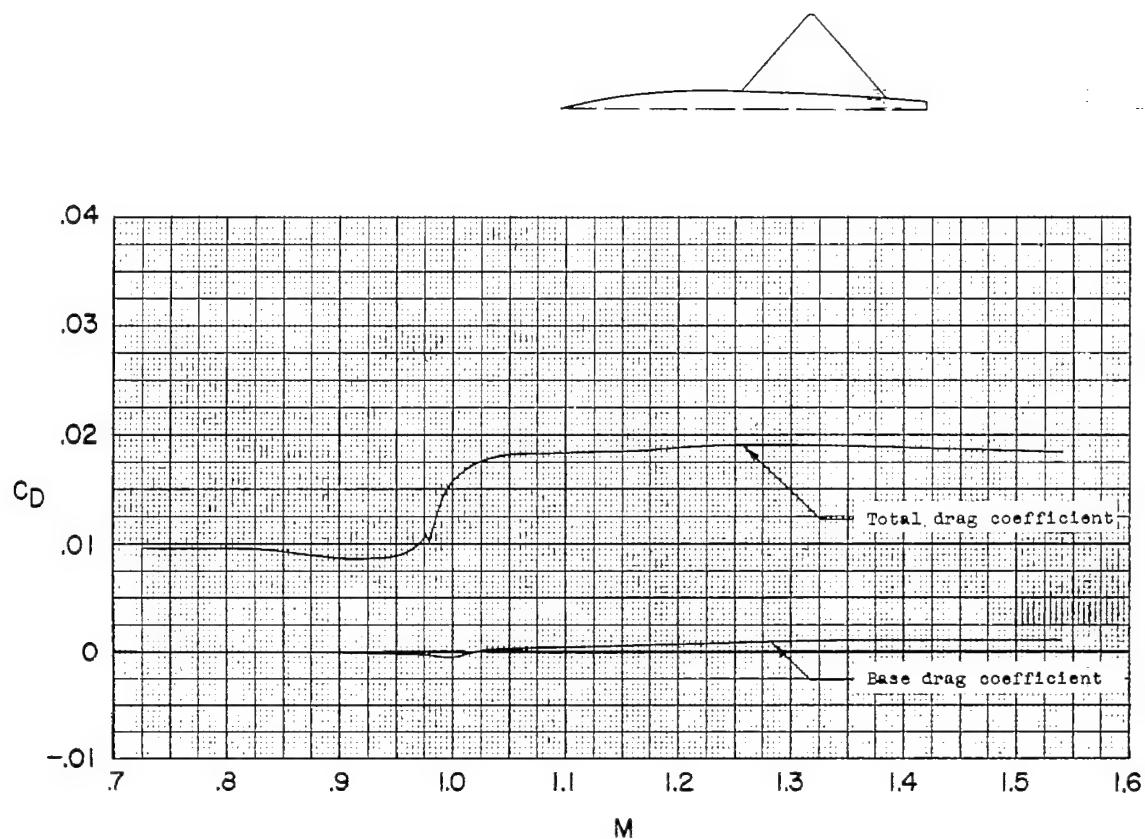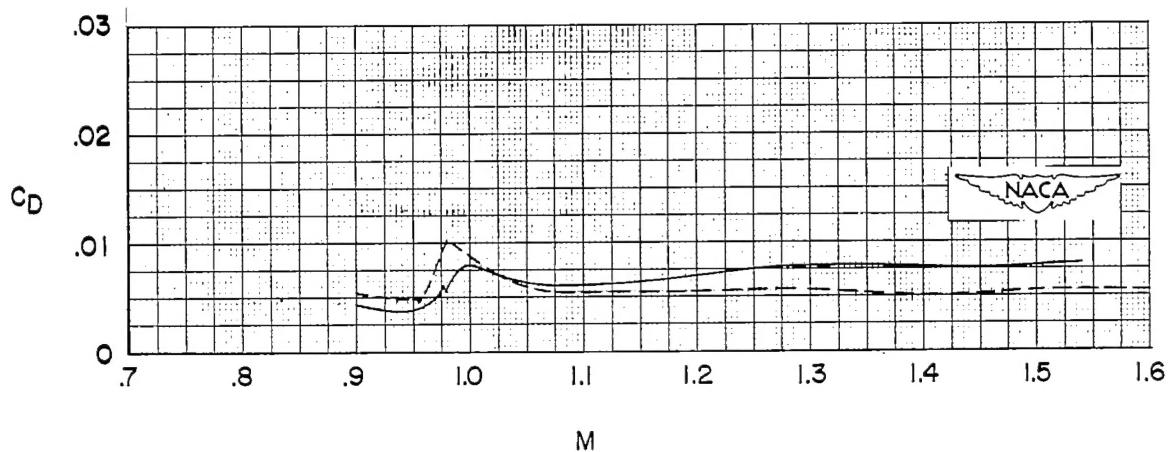
(a) Measured drag coefficients.

(b) Measured base pressure coefficient.

Figure 4.- Test data obtained for the diamond-wing model.
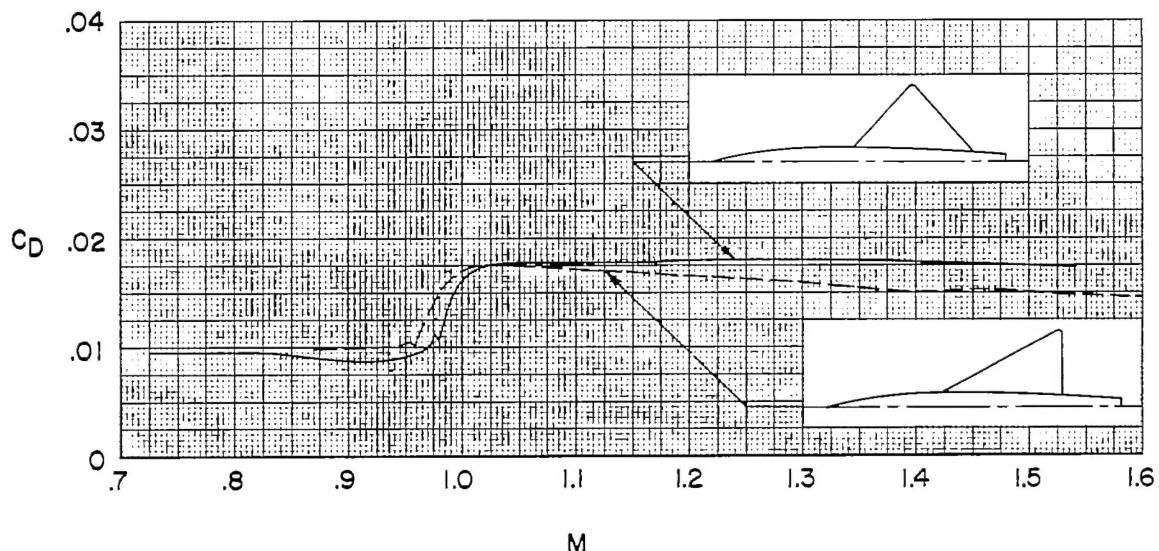
(a) Model foredrag coefficients (total drag minus base drag).

(b) Wing-plus-interference drag coefficients.

Figure 5.- Comparison of the zero-lift-drag results of a 3-percent-thick
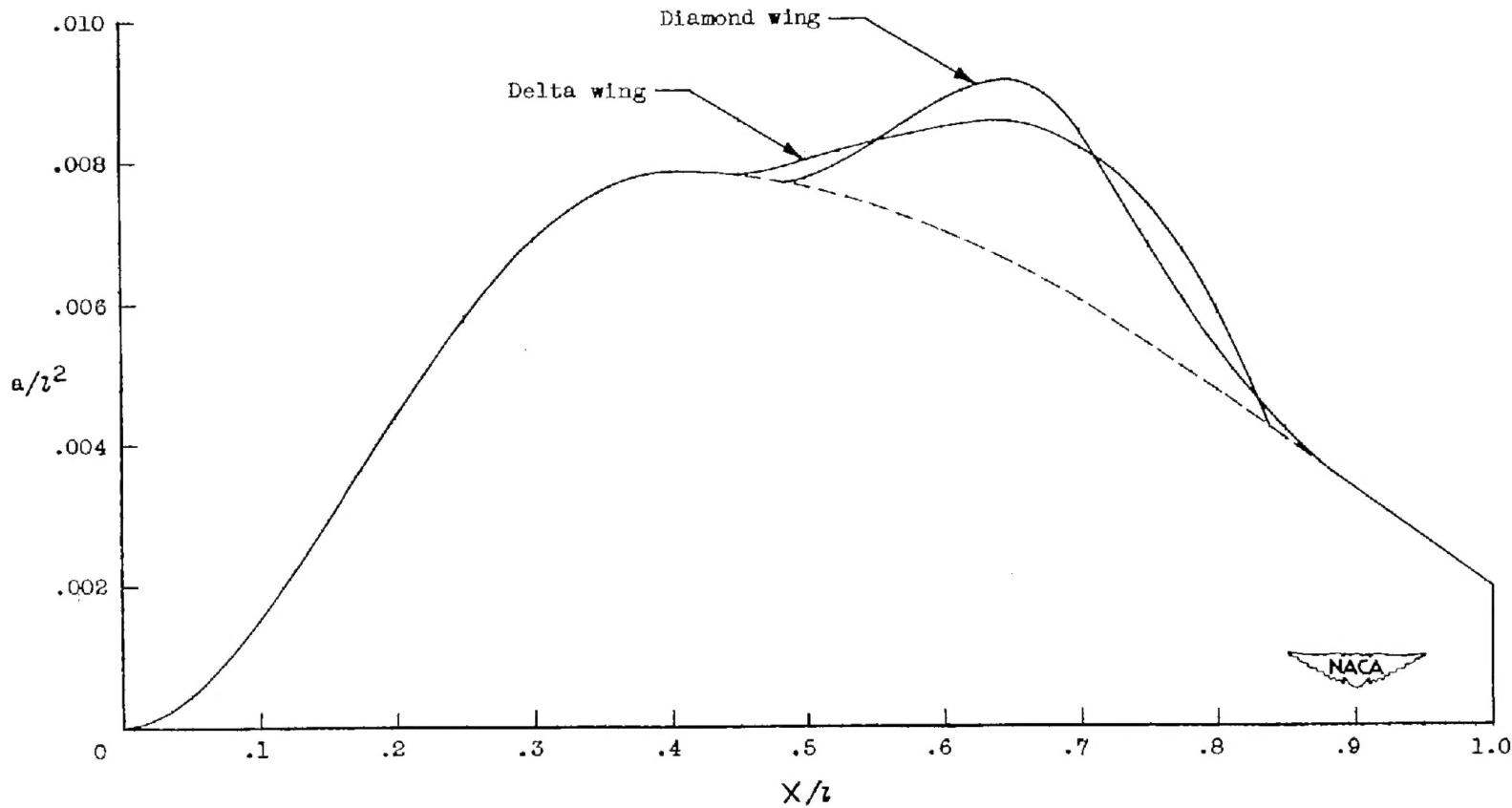diamond-wing model with a 3-percent-thick 60° delta-wing model.

Figure 6.- Longitudinal distribution of cross-sectional area for the diamond- and delta-wing configurations (not including tail fins).
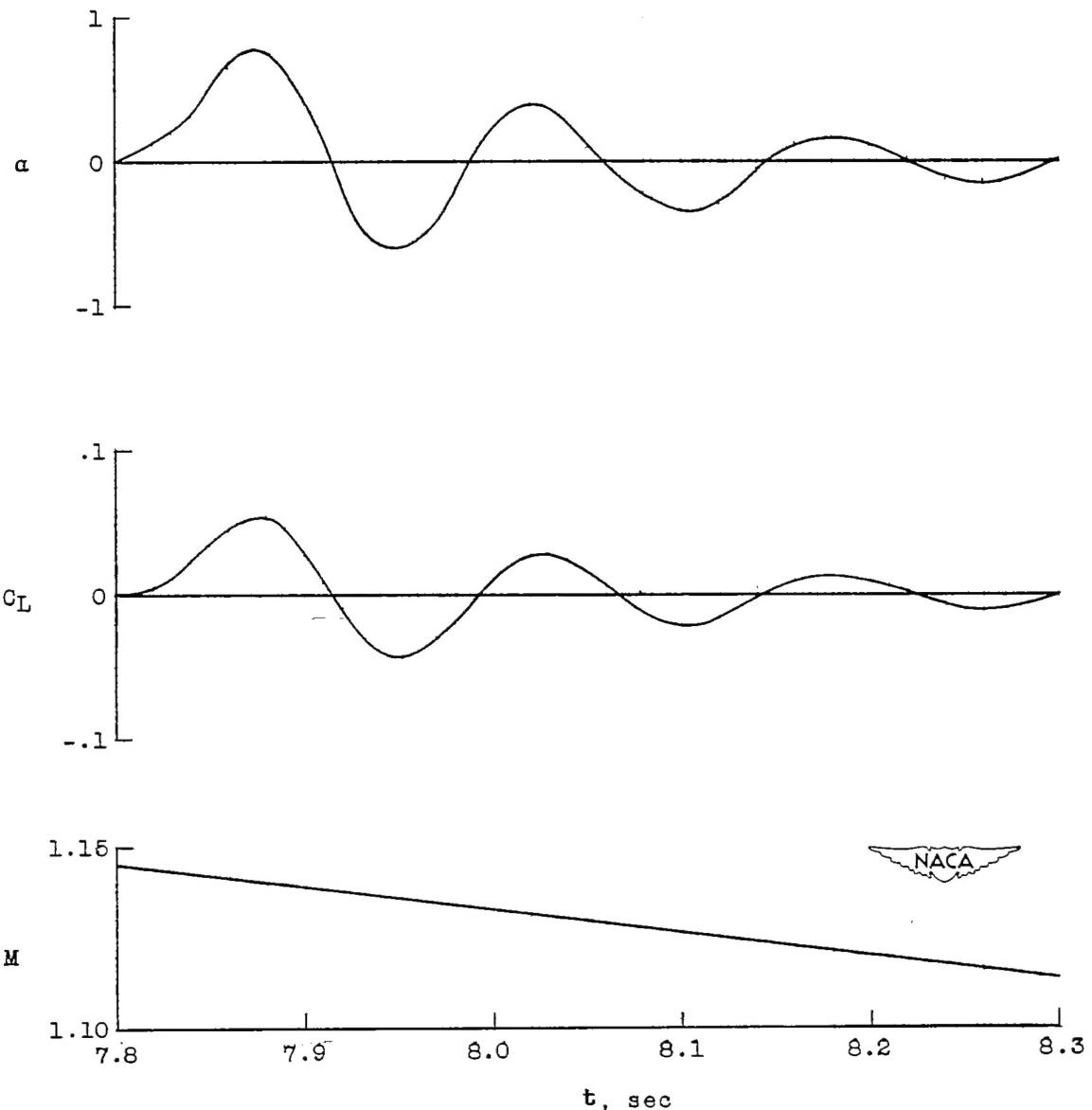
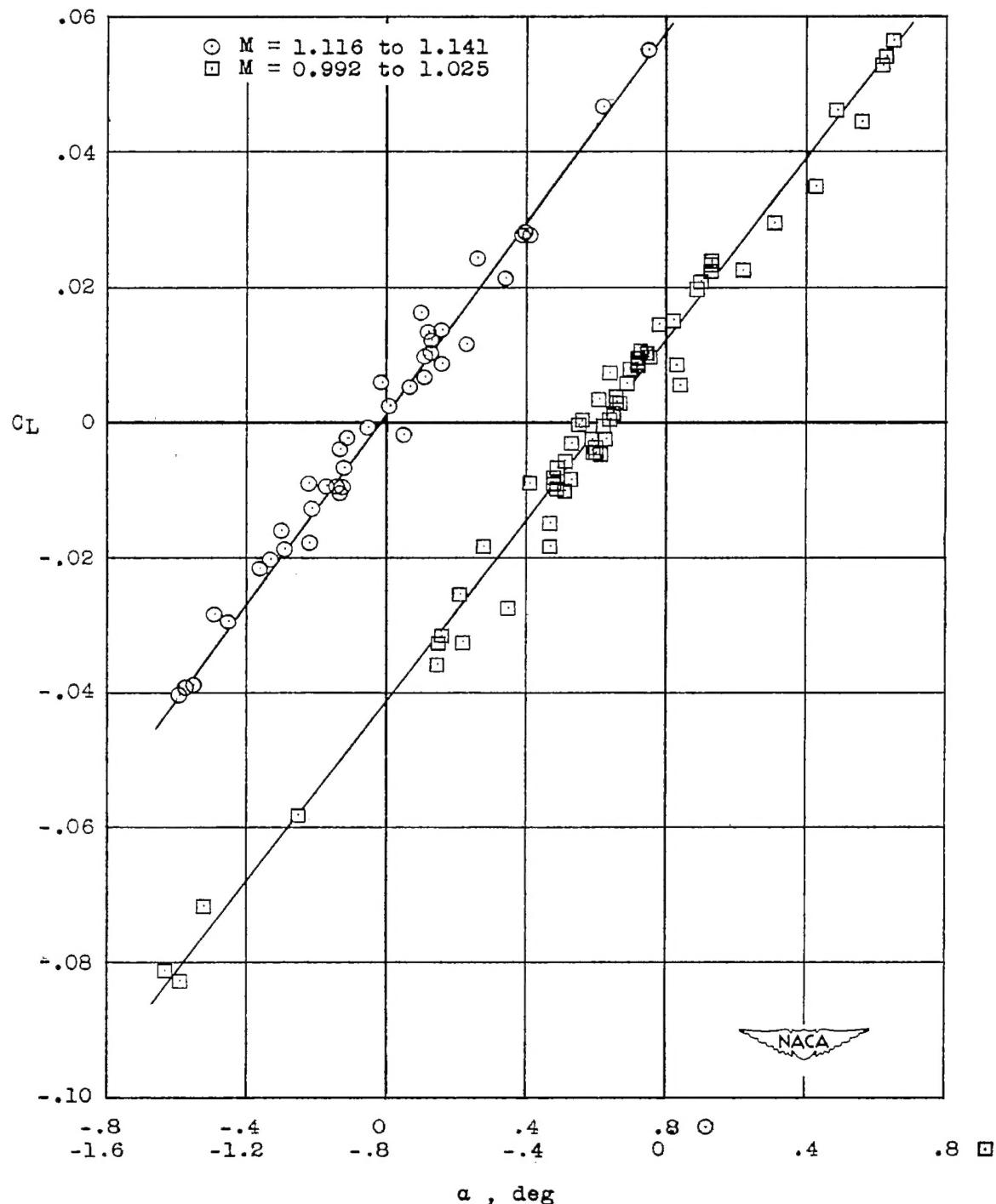Figure 7.- Portions of the time history of flight during the first pulse.

Figure 8.- Lift coefficient plotted against angle of attack for the diamond-wing model for two transonic Mach numbers.